

Title	Diode-array coupled time-resolved transmission grating spectrometer
Author(s)	Ikeda, N.; Tanaka, K.A.; Okada, K.; Mochizuki, T.; Yamanaka, C.
Citation	Review of Scientific Instruments. 57(10) P.2489-P.2492
Issue Date	1986-10
Text Version	publisher
URL	http://hdl.handle.net/11094/3269
DOI	
rights	
Note	

Osaka University Knowledge Archive : OUKA

<https://ir.library.osaka-u.ac.jp/>

Osaka University

Diode-array coupled time-resolved transmission grating spectrometer

N. Ikeda, K. A. Tanaka, K. Okada, T. Mochizuki, and C. Yamanaka

Institute of Laser Engineering, Osaka University, Yamada-Oka 2-6, Suita, Osaka 565, Japan

(Received 25 November 1985; accepted for publication 21 May 1986)

A new type of sub-keV x-ray (0.1–1.2 keV) spectrometer diode array time-resolved transmission grating spectrometer (DATTS) with a fast time response (<270 ps) has been developed to measure transient soft x-ray spectra from laser-produced plasmas. DATTS, the combination of the transmission grating (TG) and fast biplanar diodes, offers many advantages over the conventional x-ray diagnostics. Among the advantages are flexibility of the energy windows, fast time response, large dynamic range, and the capability of measuring absolute x-ray energy. All of these measurements have not been possible with a single diagnostic. The performance of the DATTS was compared with the data taken with the x-ray diode system, showing excellent agreement in the sub-keV x-ray energy range.

INTRODUCTION

X-ray spectroscopy provides indispensable information about absorption and energy transport in plasmas produced by laser irradiation of solid targets,¹ and has been a valuable diagnostic method in experiments addressing the physics relevant to laser fusion.²

Laser-produced plasmas are short lived (100 ps–1 ns), hot ($T_e = 5\text{--}6$ keV), and dense ($n_e \sim 10^{23}/\text{cm}^3$). Required information about x rays are details of spectrum, temporal history, and absolute energy in such a plasma. There are several soft x-ray diagnostics which are capable of measuring these characteristics. Among these diagnostics, filtered x-ray diodes (XRDs) are one of the most popular ones to measure the soft x-ray spectrum.^{3,4} With fast response-time diodes, it is even possible to have a temporal resolution. However, since these diodes make use of the *K* or *L* edge of the filter material, good mechanical accuracy is required for very thin (0.1–0.2 μm) filters to achieve differential data reduction. In addition, there is not much freedom to choose positions of the energy window due to the fixed energy of the *K* edges (or *L* edges). Crystal spectrometers may not be suitable for measuring the soft x-ray range below several hundred eV, since reflection efficiencies are poor in this energy range.⁵ Grating-type spectrometers are also widely used. Their reflectivity is sensitive to surface conditions. The detection of the dispersed soft x-ray spectra by either crystal or grating spectrometers is achieved with x-ray diodes or with an x-ray film. It is well known that film calibrate for an entire

soft x-ray spectral range, with proper experimental conditions, is not a simple process.⁶ A combination of an x-ray streak camera and transmission grating (TG) can also provide time resolved information about sub-keV x-ray spectra. One drawback for this system is that the dynamic range is considerably less than that of the x-ray diodes. X-ray calorimeters have the same problems as with the x-ray diodes when used with x-ray filters. It is not possible for the x-ray calorimeters to have time resolution of a laser-produced plasma since they have typically microsecond time response.⁷ In addition the sensitivity of the x-ray calorimeters is low because they make use of the heat effect rather than quantum effect of the detector material.

In the present work, a new type of sub-keV spectrometer is developed which is a combination of biplanar x-ray diodes and a transmission grating spectrometer. A diode-array coupled time-resolved transmission grating spectrometer (DATTS) features the flexible spectral windows of the TG, and the relatively large dynamic range of the biplanar diodes. Section I describes the DATTS system. Data obtained with the new instrument are presented and compared with the data measured with the XRDs in Sec. II.

I. DATTS SYSTEM

Figure 1 shows the design concept of a DATTS. The x-ray source is generated by irradiating laser light onto a solid target. The plasma electron blow-off is deflected by the

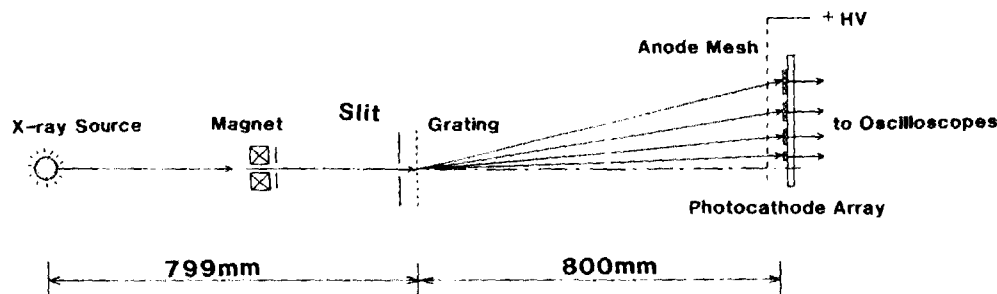


FIG. 1. Conceptual design of DATTS. Laser-produced plasma emits x rays. Plasma blow-off is deflected by the bending magnet. X rays are dispersed by the transmission grating, hit the photocathode, and are converted to electrical signal.

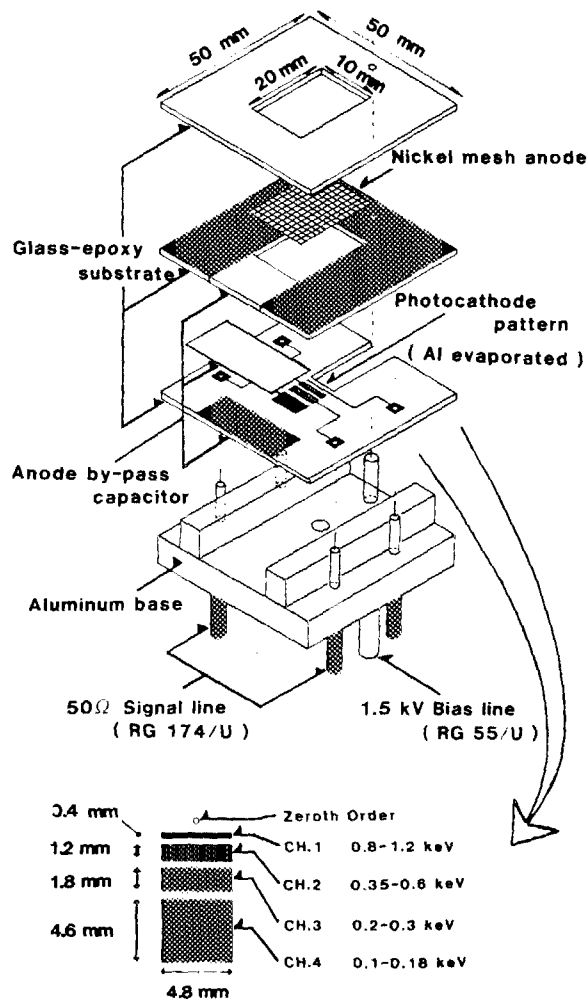


FIG. 2. Photocathode assembly. Photocathodes are photoetched on the glass-epoxy substrate and are coated with aluminum. A nickel mesh forms the anode. The bias voltage is 1.5 kV. Anode by-pass capacitor is shown, which supplies the fast rise current for the photodiodes.

bending magnet. X rays are dispersed by the TG and are collected by the photocathode array. In this experiment, the laser system delivers energies of 5–10 J in a 250-ps pulse width at 530-nm wavelength, producing intensities up to a few times 10^{14} W/cm². Targets are planar Au. Details of the x ray and plasma properties are available in Ref. 4. The magnet is located in front of the TG for protection from the plasma blow-off damage. One kgauss of magnetic field was sufficient to guard the TG from the ion blow-off. No damage was observed on the TG after this series of experiments. X rays are collimated by the slit (150 μ m) and then deflected by the TG. The TG has 1000 lines/mm with 50% opening. For a 100- μ m x-ray source, the spectral resolution of the TG is estimated to be 10 Å. The diffraction efficiency is about 10%.⁸ The dispersed x rays incident on the photocathode array are converted to an electrical signal. The diode-array assembly is shown in Fig. 2. An approximate dimension of the assembled diode array is 50×50×25 mm. The cathode pattern was made on a Cu-glass epoxy substrate by photo etching. The aluminum (2 μ m) was coated onto the cathode pattern with a properly shaped mask. The anode-cathode voltage is 1.5 kV, and was chosen taking into account the space charge limit. In the current system, four channels of cathodes correspond to energy windows of 0.1–0.18, 0.2–0.3, 0.35–0.6, and 0.8–1.2 keV. The rise time of the DATTS are a function of several factors: time dispersion of secondary electrons from the cathode, inductance and capacitance of the circuit, and transit time of secondary electrons between the electrodes. Following the expression in Ref. 9 the rise time due to the time dispersion should be less than 10 ps. With a secondary electron current, self-inductance is generated in the circuit. This inductance and an effective capacitance between electrodes also limit the rise time. Using a first-order estimation of the inductance and capacitance, the rise time due to these circuit constants should be less than

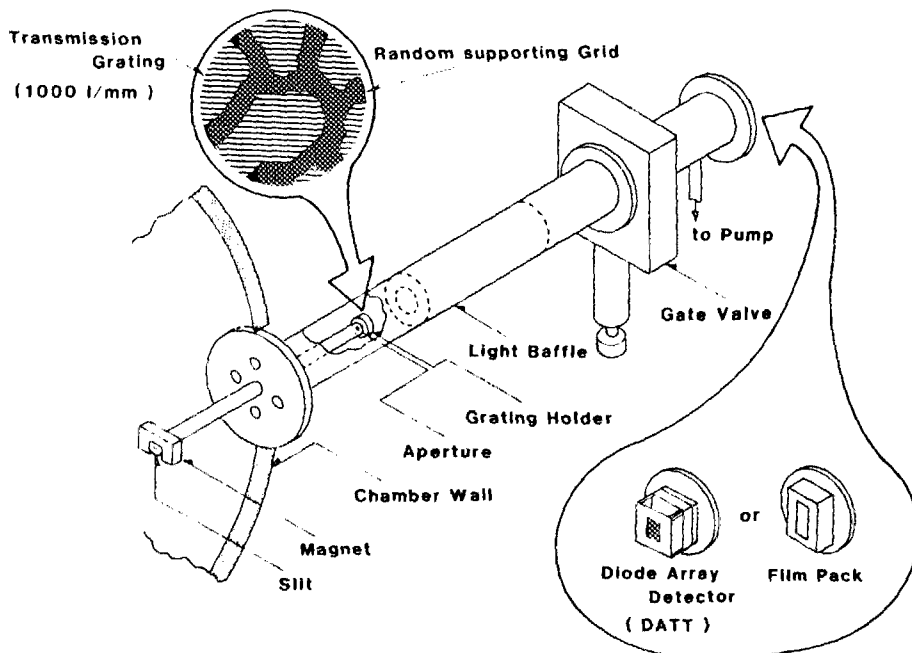


FIG. 3. Experimental geometry of DATTS. A light baffle is placed after the grating. With a gate valve, either diode array or film pack can be chosen without breaking the main chamber vacuum.

30–40 ps. More details of this type of the rise time is described in the Appendix. The secondary electrons traveling between two electrodes form an image current in the circuit, proportional to qv_e , where q and v_e are the electron charge and the speed of electrons, respectively. When the x rays hit the cathode secondary electrons are ejected and have a relatively small speed.⁹ These electrons then will gain more speed from an applied electric field, which corresponds to a larger magnitude of the current.¹⁰ Thus the electrons departing from the cathode and arriving to the anode degrade the rise time. The transit time of electrons accelerated by the bias voltage within the cathode–anode distance ($d = 1.6$ mm) is

$$T_r = d(2m_e/q)^{1/2}V_b^{-1/2},$$

where m_e is the electron mass and V_b is the bias voltage. Using $V_b = 1.5$ kV, one obtains T_r to be 140 ps. The decay time is determined by RC time constant of the circuit. The capacitance was calculated using a space charge limit current between electrodes and the bias voltage. The decay time is estimated to be ~ 130 ps. Thus the pulse width could be less than 270 ps in DATTS, and is shorter than the time response of the oscilloscope (Tektronix 7104).¹¹ Cables used for the signal lines are RG 174/U ($R = 50 \Omega$). The overall temporal response is degraded, mainly by the oscilloscope, to about 380 ps.

Figure 3 shows an actual experimental geometry of the DATTS. In the set-up, a light baffle is added after the TG. Using the gate valve, a diode array, or a film pack can be introduced without breaking the main chamber vacuum. Recording the spectrum on the calibrated film, we can compare this spectrum with that deduced from the DATTS. The film pack was used also to check the alignment of the DATTS.

III. RESULTS

In the performance-test experiment, 10-channel filtered x-ray diodes and the DATTS were symmetrically placed with respect to the laser axis. Au targets were irradiated at a

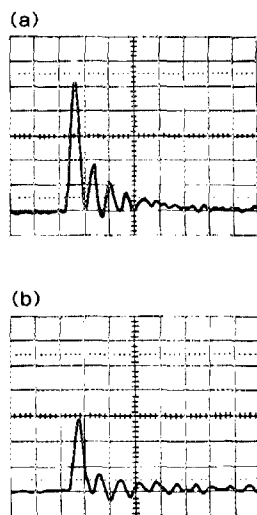


FIG. 4. Typical signals from DATTS. (a) Channel 1 signal, (b) channel 2 signal at 100 mV and 2 ns/division. Both signals show a rise time limited by an oscilloscope frequency response (380 ps).

100 mV and 2 ns/div.

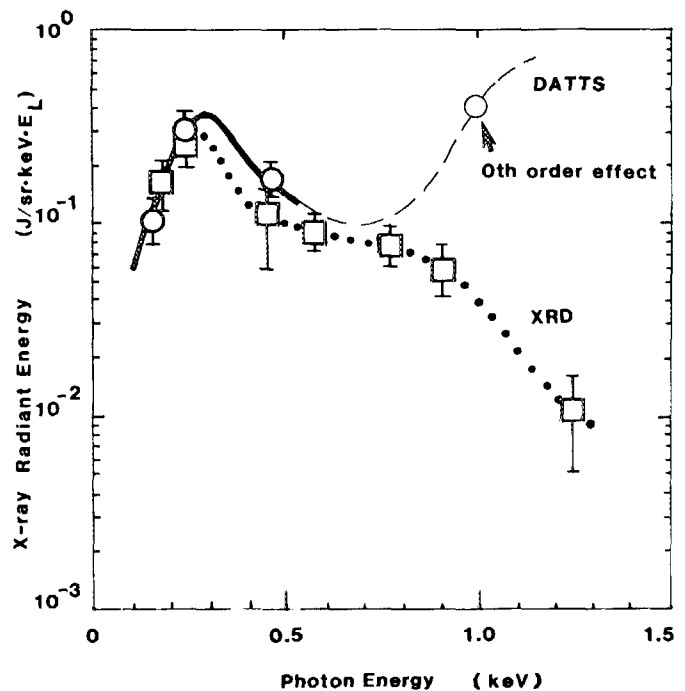


FIG. 5. X-ray spectra from DATTS and XRD systems. A line indicates the soft x-ray spectrum from the DATTS. The highest-energy channel is affected by the zeroth-order flux, thus deviating from the curve (broken line). Dotted points are the spectrum from the XRD system. In the 200–500-eV region, the DATTS spectrum shows an excellent agreement with the XRD spectrum. Positions (photon energy) of open circles indicate the center of each photocathode energy windows.

(54° incidence angle) by a 530-nm laser. Figures 4(a) and 4(b) show the typical signals from channel 1 (0.8–1.2 keV) and channel 2 (0.35–0.6 keV), both showing the rise time of about 380 ps. The temporal ringing after the peak is probably due to the fact that the coaxial cable is not directly coupled to the photocathode. Absolute energy flux at each channel of either DATTS or XRD can be calculated from the signal level taking into account the quantum efficiency of the detectors.⁴ Since the data reduction has been established for the XRD,⁴ we compare the DATTS result with that from the XRD. Figure 5 shows the soft x-ray spectra deduced from the DATTS and the XRD systems. Excellent agreement in

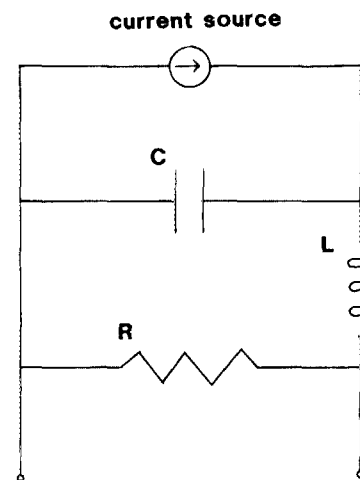


FIG. 6. Equivalent circuit of the DATTS. Capacitance (C) is at the two electrodes. Resistance (R) is determined by a cable and oscilloscope. Inductance (L) is generated with the signal current.

two spectra is readily seen except in the highest channel of the DATTS. This signal level (800–1200 eV) from the DATTS is almost one order of magnitude higher than the XRD signal level. This channel is closest to the zeroth order diffraction of the TG and is affected by this strong flux. This could be improved by shifting the entire energy range to lower energies or using a higher dispersion grating.

APPENDIX

Figure 6 shows an equivalent circuit of the DATTS. Current is generated by x-ray photoemissions and induce a magnetic field. This magnetic field creates a self-inductance (L) in the circuit. An effective capacitance (C) is introduced by the electrodes. Resistance (R) is given by the a cable and an oscilloscope impedance. Thus the rise time of this circuit is basically determined by the time constant of L/R and $1/RC$. An effective inductance is estimated to be of the order of 10^{-9} henry.

¹B. Yaakobi, J. Delettrez, L. M. Goldman, R. L. McCrory, R. Marjoribanks, M. C. Richardson, D. Shvarts, S. Skupsky, J. M. Soures, R. Hutchinson, and S. Letzring, *Phys. Fluids* **27**, 516 (1984).

²H. G. Ahlstrom, *Appl. Opt.* **20**, 1902 (1981).

³R. Kodama, K. Okada, N. Ikeda, M. Mineo, K. A. Tanaka, T. Mochizuki, and C. Yamanaka, *J. Appl. Phys.* **59**, 3050 (1986).

⁴T. Mochizuki, T. Yabe, K. Okada, M. Hamada, N. Ikeda, S. Kiyokawa, and C. Yamanaka, *Phys. Rev. A* **33**, 525 (1986); R. H. Day and P. Lee, *J. Appl. Phys.* **52**, 6965 (1981).

⁵A. Burek, D. M. Barrus, and R. L. Blake, *Astrophys. J.* **191**, 533 (1974).

⁶B. L. Henke, S. L. Kwok, J. Y. Ueji, H. T. Yamada, and G. C. Young, *J. Opt. Soc. Am. B* **1**, 818 (1984).

⁷N. Ikeda, S. Sakabe, H. Shiraga, H. Okada, M. Hamada, T. Mochizuki, and C. Yamanaka, *Technology Report Osaka Univ.* [**34**, 69 (1983), unpublished].

⁸N. M. Ceglio, R. L. Kauffman, A. M. Hawryluk, and H. Medeck, *Appl. Opt.* **22**, 318 (1983).

⁹B. L. Henke, *Nucl. Instrum. Methods* **177**, 161 (1980).

¹⁰When an electron moves from the cathode to the anode, a charge is induced on the electrodes producing a current. The current is expressed as $i = dQ/dt \propto qv$, where Q is the total charge induced on each of the electrodes. Since the electron is accelerated by a bias voltage, $i(t)$ is proportional to time until the electron arrives at the anode.

¹¹Tektronix Catalogue (1982, unpublished).